

USING IONOSPHERIC CURRENTS TO INFER IONOSPHERIC ELECTRIC FIELDS AND THERMOSPHERIC WINDS FROM MAVEN OBSERVATIONS

M. O. Fillingim, A. Fogle, P. Dunn, J. P. McFadden, *Space Sciences Laboratory, University of California, Berkeley, CA, USA (matt@ssl.berkeley.edu)*, J. E. P. Connerney, P. R. Mahaffy, M. Benna, *NASA Goddard Space Flight Center, Greenbelt, MD, USA*, R. E. Ergun, L. Andersson, *Laboratory for Atmospheric and Space Physics, University of Colorado, Boulder, CO, USA*.

Introduction:

How the solar wind interacts with a planetary object depends upon the object's properties, such as the presence of a magnetic field or an atmosphere. An unmagnetized object cannot stand-off the solar wind unless it possess a substantial atmosphere. Currents can be induced in the ionosphere which act to cancel out the external solar wind magnetic field preventing it from reaching the surface. Here we present observations of such induced currents in the ionosphere of Mars and infer the possible drivers that support these currents.

Data and Methodology:

Magnetic fields and currents: During its elliptical, approximately 4.5-hour orbit, MAVEN repeatedly passes through the upper ionosphere providing in-situ measurements of the magnetic field throughout the ionosphere of Mars. From these local measurements, we calculate ionospheric currents from the curl of the magnetic field using Ampère's Law: $\mathbf{j} = 1/\mu_0 \nabla \times \mathbf{B}$. In spherical coordinates, this becomes

$$\mathbf{j} = \frac{1}{\mu_0} \left[\frac{1}{r \sin \theta} \left(\frac{\partial}{\partial \theta} (B_\phi \sin \theta) - \frac{\partial B_\theta}{\partial \phi} \right) \hat{r} + \frac{1}{r} \left(\frac{1}{\sin \theta} \frac{\partial B_r}{\partial \phi} - \frac{\partial}{\partial r} (r B_\phi) \right) \hat{\theta} + \frac{1}{r} \left(\frac{\partial}{\partial r} (r B_\theta) - \frac{\partial B_r}{\partial \theta} \right) \hat{\phi} \right]$$

However, since we only have one spacecraft, we have to make assumptions about the uniformity of the magnetic field and the direction of magnetic field gradients. We assume that the principle gradient in the magnetic field is in the radial direction and that gradients in the theta and phi (horizontal) directions are negligible. This assumption is most likely satisfied when the magnitude and variation of radial component of the magnetic field are small compared to the magnitude and variation of the theta and phi components. Under this assumption, the above equation reduces to

$$\mathbf{j} \approx \frac{1}{\mu_0} \left[\frac{1}{r} \left(-\frac{\partial}{\partial r} (r B_\phi) \right) \hat{\theta} + \frac{1}{r} \left(\frac{\partial}{\partial r} (r B_\theta) \right) \hat{\phi} \right]$$

In an attempt to satisfy this assumption, we restrict our analysis to a subset of the MAVEN magnetic field

data where the ionospheric magnetic fields are approximately horizontal to the surface; i.e., the radial component of the magnetic field is small. Therefore, when computing ionospheric currents, we only use magnetic field data with a magnetic dip angle (the angle between the magnetic field direction and the horizontal) less than 18° between 300 km altitude and the spacecraft periapsis (~ 150 km altitude). The calculated ionospheric currents are likewise horizontal (the computed currents only have theta and phi components as indicated by the above equation).

Figure 1 shows the MAVEN magnetic field measurements from the MAG instrument [1] (left) as well as the currents computed from these measurements using the above assumptions and equations (right).

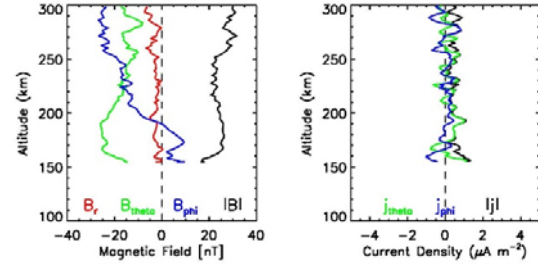


Figure 1: Left panel: MAVEN MAG observations of the ionospheric magnetic field from 300 km altitude to periapsis corresponding to 13:41:52 – 13:49:08 UT on 2016-04-14. Right panel: horizontal ionospheric currents calculated from the observed magnetic field.

At high altitude, above ~ 250 km, the magnetic field is westward (B_ϕ is positive eastward) with a northward component (B_θ is positive southward) consistent with a draped interplanetary magnetic field. As the altitude decreases, the magnetic field rotates northward. The magnitude of the field remains fairly constant until the spacecraft approaches periapsis near 150 km where the magnitude decreases by a factor of ~ 2 . Throughout this altitude range, the radial component of the magnetic field is small ($|B_r| < \sim 5$ nT), and the maximum dip angle is 14° , satisfying our horizontal field requirement.

At high altitude, where the magnetic field magnitude and direction are relatively constant, the associated currents are relatively weak. Around 200 km, where the magnetic field is rotating, there is a southward current (j_θ) with magnitude of $\sim 1 \mu\text{A m}^{-2}$. The

magnitude of the current increases again near periapsis where the magnitude of the magnetic decreases. We should note that below 200 km, the magnetic field direction is predominantly in the northward (negative B_θ) direction. Currents in the theta (north-south) direction, at about 200 km and near periapsis, are therefore parallel or anti-parallel to the horizontal magnetic field. This is in contrast to the terrestrial case where field aligned currents are typically thought to be vertical.

Current drivers: Once we determine the currents, we can investigate what processes support these currents in the ionosphere. Starting with the steady state ion and electron equations of motion, neglecting ion-electron collisions,

$$-\frac{1}{n_{i,e}} \nabla(n_{i,e} k T_{i,e}) + m_{i,e} \mathbf{g} \pm q(\mathbf{E} + \mathbf{v}_{i,e} \times \mathbf{B}) - m_{i,e} v_{in,en}(\mathbf{v}_{i,e} - \mathbf{u}) = 0$$

where n is the particle density, k is Boltzmann's constant, T is temperature, m is particle mass, \mathbf{g} is the acceleration due to gravity, q is the absolute value of the particle charge, \mathbf{E} is the electric field, \mathbf{v} is the particle velocity, \mathbf{B} is the magnetic field, v is the particle-neutral collision frequency, \mathbf{u} is the neutral (thermospheric) wind velocity, and the subscripts i and e correspond to ions and electrons, respectively, we can solve for the particle velocity in terms of the forces in both the parallel and perpendicular directions:

$$\mathbf{v}_{s\parallel} = \left(\frac{1}{m_s v_{sn}} \right) \mathbf{F}_{s\parallel} + \mathbf{u}_{\parallel}$$

and

$$\mathbf{v}_{s\perp} = \left(\frac{1}{m_s v_{sn}} \right) \left(\frac{v_{sn}^2}{v_{sn}^2 + \omega_s^2} \right) \left(\mathbf{F}_{s\perp} \pm \frac{\omega_s}{v_{sn}} \mathbf{F}_{s\perp} \times \hat{\mathbf{b}} \right) + \mathbf{u}_{\perp}$$

where

$$\mathbf{F}_s = -\frac{1}{n_s} \nabla(n_s k T_s) + m_s \mathbf{g} \pm q(\mathbf{E} + \mathbf{u} \times \mathbf{B})$$

ω is the particle gyrofrequency, and s represents ions and electrons.

The current density is given by

$$\mathbf{j} = nq(\mathbf{v}_i - \mathbf{v}_e)$$

By ignoring the pressure gradient and gravity terms in the force expression and plugging the ion and electron velocity expressions into the current equation, we can express the parallel and perpendicular currents as functions of the electric field and neutral wind velocity:

$$\mathbf{j}_{\parallel} = \sigma_{\parallel}(\mathbf{E} + \mathbf{u} \times \mathbf{B}) = \sigma_{\parallel} \mathbf{E}_{\parallel}$$

and

$$\mathbf{j}_{\perp} = \sigma_P(\mathbf{E} + \mathbf{u} \times \mathbf{B}) - \sigma_H(\mathbf{E} + \mathbf{u} \times \mathbf{B}) \times \hat{\mathbf{b}}$$

where

$$\begin{aligned} \sigma_{\parallel} &= \frac{n_i q_i^2}{m_i v_{in}} + \frac{n_e q_e^2}{m_e v_{en}} \\ \sigma_P &= \frac{n_i q_i^2}{m_i v_{in}} \left(\frac{v_{in}^2}{v_{in}^2 + \omega_i^2} \right) + \frac{n_e q_e^2}{m_e v_{en}} \left(\frac{v_{en}^2}{v_{en}^2 + \omega_e^2} \right) \\ \sigma_H &= -\frac{n_i q_i^2}{m_i v_{in}} \left(\frac{v_i \omega_i}{v_{in}^2 + \omega_i^2} \right) + \frac{n_e q_e^2}{m_e v_{en}} \left(\frac{v_{en} \omega_e}{v_{en}^2 + \omega_e^2} \right) \end{aligned}$$

are the parallel (or direct), Pedersen, and Hall conductivities, respectively.

For simplicity, we consider two end members as current drivers: electric fields and neutral winds. Assuming the currents are driven by electric fields, the driving force becomes $\mathbf{F} = \pm q\mathbf{E}$ and $\mathbf{u} = 0$. Solving the current equations for the electric field gives the standard, simplified Ohm's Law:

$$\mathbf{E}_{\parallel} = \frac{\mathbf{j}_{\parallel}}{\sigma_{\parallel}}$$

and

$$\mathbf{E}_{\perp} = \frac{\sigma_P}{\sigma_P^2 + \sigma_H^2} \left(\mathbf{j}_{\perp} + \frac{\sigma_H}{\sigma_P} \mathbf{j}_{\perp} \times \hat{\mathbf{b}} \right)$$

Alternatively, assuming that the currents are driven by neutral winds, the driving force becomes $\mathbf{F} = \pm q(\mathbf{u} \times \mathbf{B})$ and $\mathbf{E} = 0$. Solving the current equation for the neutral wind gives

$$\mathbf{u}_{\perp} = \frac{1}{B} \frac{\sigma_P}{\sigma_P^2 + \sigma_H^2} \left(\frac{\sigma_H}{\sigma_P} \mathbf{j}_{\perp} - \mathbf{j}_{\perp} \times \hat{\mathbf{b}} \right)$$

In steady state, a parallel neutral wind cannot support a parallel current: positive and negative particles move in the same direction at the same speed, so there is not differential motion. Therefore, from observations of currents, we are unable to derive any information about neutral winds parallel to the ambient magnetic field.

In order to quantitatively estimate the current drivers, we need to first compute the conductivities. We can compute the conductivities given knowledge of the thermospheric (neutral) composition, density, and temperature as well as the ionospheric composition, density, and temperature and the magnetic field magnitude.

Figure 2 shows the neutral composition and density as measured by the Neutral Gas and Ion Mass Spectrometer (NGIMS) [2] (left) and the ion composition and density from the Suprathermal and Thermal Ion Composition (STATIC) instrument [3] and the electron density from the Langmuir Probe and Waves (LPW) instrument [4] (right) for the same interval shown in Figure 1.

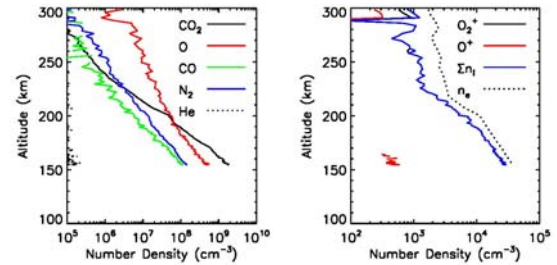


Figure 2: Left panel: MAVEN NGIMS neutral composition and density observations. Right panel: MAVEN STATIC and LPW observations of ion composition and density and electron density. The time interval is the same as that shown in Figure 1.

In the right panel of Figure 2, we can see that throughout most of the altitude range, STATIC does not return usable O^+ densities. Where O^+ densities are

reported, at the topmost and bottommost altitudes (red curve), the O^+ density is a small fraction of the O_2^+ density. Also note that there is good agreement between the total ion density (blue curve), which is simply the O_2^+ density throughout most of the altitude range, and the electron density (dotted curve). Therefore, where O^+ densities are not reported, we assume that all ions are O_2^+ .

From the ion composition and magnetic field magnitude, we compute particle gyrofrequencies, $\omega_{i,e}$. From the neutral composition, the neutral, ion, and electron temperatures, and collision frequency expressions (given by [5], for example), we compute the ion-neutral and electron-neutral collision frequencies, $\nu_{in,en}$. We note that, since we do not have measurements of neutral temperatures, we assume that the ion and neutral temperatures are equal below 180 km and that the neutrals are isotropic above this altitude.

The parallel (direct), Pedersen, and Hall conductivities calculated using the above data and assumptions are shown in Figure 3.

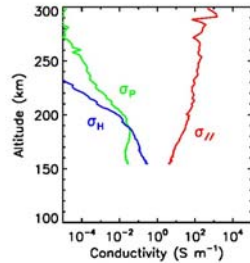


Figure 3: Parallel (direct), Pedersen, and Hall conductivities, as defined in the text, calculated from MAVEN observations.

Once we have the conductivities and currents, we are able to compute the possible current drivers. Figure 4 shows the computed electric field assuming neutral winds are zero. The left hand panel shows the perpendicular and parallel components of the electric field. The parallel component (in red) has been multiplied by a factor of 100 for clarity. The right hand panel shows the perpendicular component of the electric field in spherical coordinates.

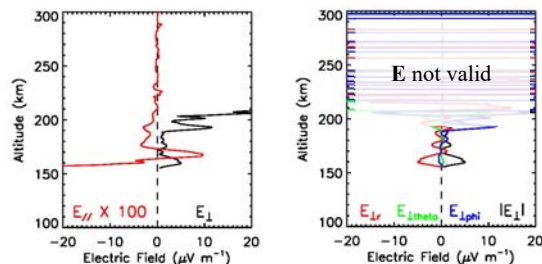


Figure 4: Left panel: Parallel (red) and perpendicular components of the electric field calculated from conductivities and currents. Right panel: Perpendicular component of the electric field in spherical coordinates. Above ~ 200 km, the calculated electric field is not valid.

It is important to note that the calculated electric field is not valid above ~ 200 km. Above this altitude, the electric field becomes unphysically large as the conductivities become very small. In this high altitude region, both the ions and electrons are magnetized and are no longer collisionally coupled to the neutrals. The above expressions relating the electric field to the current were derived assuming a collisional ionosphere. In a non-collisional regime, an electric field will cause the ions and electrons to drift together, and a current will not be generated. The simplified version of Ohm's Law is no longer applicable.

At lower altitudes, the perpendicular component of the electric field is typically a few microVolts per meter. The parallel component is approximately 100 times smaller, on the order of $0.1 \mu V m^{-1}$. Since the parallel conductivity is much larger than the Pedersen or Hall conductivities, the parallel electric field is similarly much smaller than the perpendicular electric field. Near periapsis, we can see that the perpendicular component of the electric field is predominantly in the radial direction. Since the Hall conductivity is larger at these altitudes (see Figure 3), a radial electric field will drive a horizontal Hall (electron) current.

Figure 5 shows the perpendicular thermospheric neutral winds computed from the conductivities and currents assuming the electric field is zero. The left panel shows the magnitude of the perpendicular neutral winds (we have no information about parallel neutral winds, see above), and the right panel shows the perpendicular neutral winds in spherical coordinates.

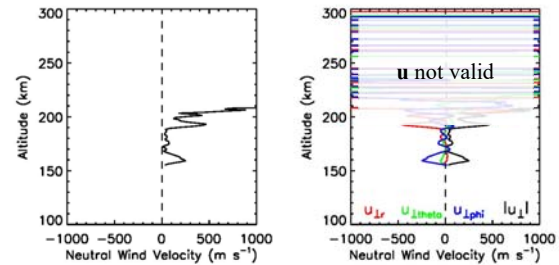


Figure 5: Left panel: Magnitude of the perpendicular thermospheric neutral winds. Right panel: Perpendicular neutral winds in spherical coordinates. Above ~ 200 km, the calculated neutral winds are not valid.

As is the case for the electric fields, the computed neutral winds are not valid above ~ 200 km since neither the ions nor electrons are collisional. The peak magnitude of the neutral winds near periapsis is ~ 250 m/s. The neutral winds are predominantly westward (negative phi direction) near periapsis. However, since the magnetic field is predominantly northward near periapsis (see Figure 1), we do not have any information about neutral winds in the north-south (parallel) direction.

Summary and Future Work:

Using MAVEN observations of the magnetic field, thermospheric composition and density, and

ionospheric composition and density, we have attempted to calculate the horizontal ionospheric currents under the restriction of horizontal ionospheric magnetic fields. Then we have calculated the strength of the driving force assuming the current is driven by electric fields and, separately, assuming the current is driven by thermospheric neutral winds. We find that the electric fields necessary to drive the calculated currents are on the order of a few microVolts per meter predominantly in the radial direction. The neutral winds necessary to drive the current are on the order of a few hundred meters per second in the horizontal direction.

The obvious next steps are to compare our estimates of electric fields and thermospheric winds to global models. High resolution models of the Mars-solar wind interaction may reveal predicted electric field structure in the ionosphere. Similarly, atmospheric circulation models can predict thermospheric wind velocities and directions. By comparing data-derived parameters with model predictions, we can try to determine the predominant drivers of the ionospheric currents.

Additionally, only one passage of the spacecraft has been shown here. Future work will also consider many more orbits to build up a map of the magnitude and direction of the possible current drivers.

References:

- [1] Connerney, J. E. P., J. Espley, P. Lawton, S. Murphy, J. Odom, R. Oliverson, and D. Sheppard (2015), The MAVEN magnetic field investigation, *Space Sci. Rev.*, 195(1), 257-291, doi:10.1007/s11214-015-0169-4.
- [2] Mahaffy, P. R., M. Benna, T. King, D. N. Harpold, R. Arvey, M. Barciniak, M. Bendt, D. Carrigan, T. Errigo, V. Holmes, C. S. Johnson, J. Kellogg, P. Kimvilakani, M. Lefavor, J. Hengemihle, F. Jaeger, E. Lyness, J. Maurer, A. Melak, F. Noreiga, M. Noriega, K. Patel, B. Prats, E. Raaen, F. Tan, E. Weidner, C. Gundersen, S. Battel, B. P. Block, K. Arnett, R. Miller, C. Cooper, C. Edmonson, and J. T. Nolan (2015), The neutral gas and ion mass spectrometer on the Mars atmosphere and volatile evolution mission, *Space Sci. Rev.*, 195(1), 49-73, doi:10.1007/s11214-014-0091-1.
- [3] McFadden, J. P., O. Kortmann, D., Curtis, G. Dalton, G. Johnson, R. Abiad, R. Sterling, K. Hatch, P. Berg, C. Tiu, D. Gordon, S. Heavner, M. Robinson, M. Marchwordt, R. Lin, and B. Jakosky (2015), MAVEN suprathermal and thermal ion composition (STATIC) instrument, *Space Sci. Rev.*, 195(1), 199-256, doi:10.1007/s11214-015-0175-6.
- [4] Andersson, L., R. E. Ergun, G. T. Delory, A. Eriksson, J. Westfall, H. Reed, J. McCauly, D. Summers, and D. Meyers (2015), The Langmuir probe and waves (LPW) instrument for MAVEN, *Space Sci. Rev.*, 195(1), 173-198, doi:10.1007/s11214-015-0194-3.
- [5] Schunk, R. W., and A. F. Nagy (2000), *Ionospheres: Physics, Plasma Physics, and Chemistry*, Cambridge University Press.